

# Radio-frequency size effect in tin cylinders

V. S. Tsoi

*Institute of Solid State Physics, USSR Academy of Sciences*

(Submitted November 28, 1972)

Zh. Eksp. Teor. Fiz. **64**, 2140-2147 (June 1973)

The magnetic field dependence of the derivative of the imaginary part of the surface impedance  $X$  with respect to magnetic field strength is investigated experimentally for tin cylinders with various radii and crystallographic orientations. A new type of size effect is observed: when the electron trajectory curvature is comparable with the sample radius, a singularity in  $X$  is observed. A nonlinear dependence of  $X$  in weak fields is detected.

## INTRODUCTION

Measurement of the surface impedance  $Z$  is a powerful method of investigating metals. Since the experiments are carried out on samples with limited dimensions, it is of interest to ascertain the extent to which the curvature of the surface of the investigated sample influences the final results. The influence of curvature is profitably investigated with samples of cylindrical shape. The anomalous skin effect in metallic cylinders with radii  $r \ll l$  ( $l$  is the electron mean free path) was investigated theoretically in<sup>[1]</sup>, where it was shown that  $Z$  does not depend on  $r$  in the case of diffuse reflection of the electrons from the sample surface, and that  $Z \sim r^{1/5}$  in the case of specular reflection. However,  $Z$  is strongly influenced by the law governing the reflection of the electrons from the surface: specularity of the reflection decreases  $Z$ . The study of the influence of the curvature on the dependence of  $Z$  and  $H$  has been the subject of<sup>[2-5]</sup>. In<sup>[2]</sup>, a nonmonotonic dependence of  $X$  ( $X = \text{Im } Z$ ) on the field was observed at 1.9 MHz in the case of tin cylinders with approximate radius 4 mm; this dependence has not been explained to this day. A radial-frequency size effect was observed for the first time in<sup>[3]</sup> on samples of cylindrical form (SEC). The measurements were performed on potassium under conditions  $l \gtrsim r$ . Besides the monotonic increase of  $\partial Z/\partial H$  with the field in the region  $H < H_0$  and the sharp decrease near  $H_0$  ( $H_0$  is the field at which the Larmor radius  $r_H = p_F c/eH$  is equal to  $r$ , where  $p_F$  is the Fermi momentum of the electron), impedance singularities were observed<sup>[3]</sup> at  $H = H_0, 2H_0, 3H_0, \dots$ , similar to the lines of the radio-frequency size effect (SE) in a plane-parallel plate<sup>[6]</sup>. The theory of the anomalous skin effect in metallic cylinders in a magnetic field parallel to the cylinder axis has been developed in<sup>[4]</sup>, where in the case of a quadratic dispersion law an asymptotic expression was obtained for  $\partial Z/\partial H$  as a function of  $H$  as  $\delta \rightarrow 0$  ( $\delta$  is the depth of the skin layer); this expression agreed qualitatively with the experimental relation<sup>[3]</sup> in the region  $H < H_0$ . The condition that the Fermi surface be spherical strongly limits the application of the SEC, but as shown by experiment performed on indium samples<sup>[5]</sup>, the SEC is observed also in metals with non-spherical complicated Fermi surfaces and even under the condition  $l \ll r$ .

In this article we present the results of a study of SEC on tin at frequencies 1–10 MHz.

## EXPERIMENT

**A. Procedure.** The measurements were performed on samples that were cast in polished cylindrical quartz molds. Figure 1 shows a quartz mold. The samples

| Sample           | Diameter, mm | $\theta$ , deg | $\psi$ , deg | $10^{-19}$ g-cm/sec | Sample            | Diameter, mm | $\theta$ , deg | $\psi$ , deg | $10^{-19}$ g-cm/sec |
|------------------|--------------|----------------|--------------|---------------------|-------------------|--------------|----------------|--------------|---------------------|
| KI <sup>3</sup>  | 3.4          | —              | —            | 0.80                | Sn8 <sup>5</sup>  | 5.5          | 36             | 0            | 2.7                 |
| Sn1 <sup>3</sup> | 3.4          | 36             | 40           | 1.9                 | Sn10 <sup>5</sup> | 3.4          | 34             | 30           | 1.8; 1.6            |
| Sn5 <sup>3</sup> | 3.4          | 6              | 0            | 1.9                 | Sn10 <sup>5</sup> | 5.5          | 34             | 30           | 1.8; 1.6            |
| Sn4 <sup>5</sup> | 5.0          | 10             | 15           | 2.1                 | Sn2 <sup>8</sup>  | 8.0          | 34             | 30           | 1.8; 1.6            |
| Sn6 <sup>5</sup> | 5.0          | 19             | 42           | 2.7                 |                   |              |                |              |                     |

Note.  $\theta$  is the angle between the cylinder axis and the [001] fourfold axis of the tetragonal axis of tin,  $\psi$  is the angle between the [100] twofold axis and the projection of the cylinder on a plane perpendicular to [001]. The angles  $\theta$  and  $\psi$  are determined from the etch figures accurate to  $\approx 2^\circ$ . At 4.2°K,  $l \approx 0.3$  mm in tin ( $p_l = 1.05 \times 10^{11}$  Ω-cm<sup>2</sup> [9]) and  $l \approx 0.2$  mm in potassium ( $l = p_F Ne^2/p$ ,  $p = eH^2/c$ ).

were made of tin with a ratio  $\rho(\text{room})/\rho(4.2^\circ\text{K}) \approx 40\,000$  and of potassium with  $\rho(\text{room})/\rho(4.2^\circ\text{K}) \approx 6200$  ( $\rho(\text{room})$  and  $\rho(4.2^\circ\text{K})$  are the resistivities at room temperature and at 4.2°K). The technique of growing single-crystal tin samples with specified shape and crystallographic orientation is described in<sup>[7]</sup>, and the technique for potassium in<sup>[8]</sup>. The characteristics of the samples are summarized in the table. The sample was placed inside the inductance coil of the tank circuit of a measuring oscillator in such a way that the radio-frequency currents flowed around the cylinder in an azimuthal direction; the deviation of the generation frequency  $\Delta f \sim -\Delta(X)$  and its change were recorded by a modulation method<sup>[10]</sup>. The constant magnetic field was directed along the cylinder axis.

**B. Measurement results.** The simplest dependence of the derivative  $f' \equiv \partial f/\partial H$  of the generation frequency, with respect to  $H$  for a tin cylinder is given by curve 2 of Fig. 2, without the two minima. In this case, when  $H$  is rotated through an angle  $\varphi$  in the plane containing the cylinder axis,  $f'$  is determined only by the value of  $\varphi$ . At certain crystallographic orientations of the sample, a minimum of  $f'$  is observed near  $H = 0$  (nonmonotonic dependence of  $X$ ), and the shape of the curve is not influenced by the amplitude of the high-frequency field  $H_\omega$ , which in our experiments could be varied in the interval 0.6–6.0 Oe. An additional complication was introduced by the appearance of two types of dependences of  $f'$  on  $H_\omega$  in  $H = 0$ : (1) when  $H_\omega$  was increased, the value of  $f'$  oscillated (curve 1 of Fig. 2; at  $H_\omega \lesssim 2.5$  Oe, the maximum of  $f'$  closest to  $H = 0$  dropped out from curve 1 of Fig. 2); (2) with increasing  $H_\omega$ , the minimum of  $f'$  dropped out, and a peak appeared, the "traces" of which are shown in Fig. 3 (curve 3); the peak is clearly seen in Fig. 4 (curves 1 and 2). For a number of samples, additional maxima and minima of  $f'(H)$  were observed in fields 10–100 Oe, and also the SEC lines (see Fig. 2–4, the SEC lines are marked by vertical arrows).

The impedance of the samples was exceedingly sen-

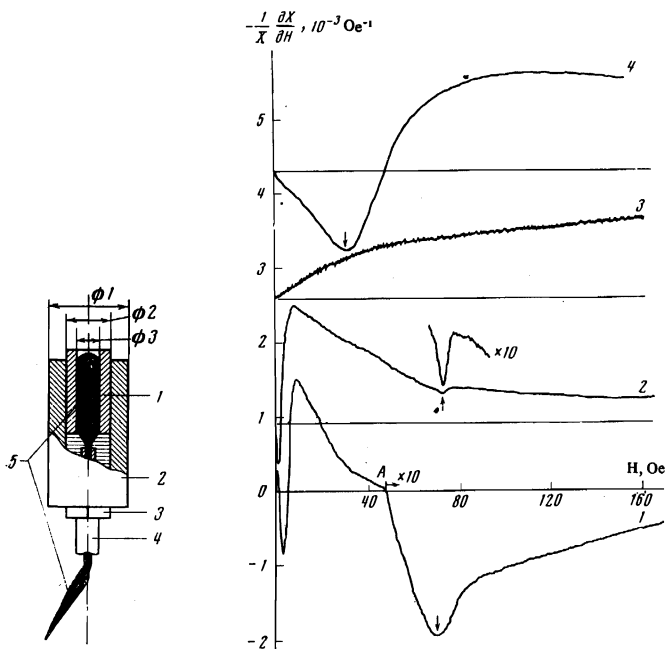


FIG. 1

FIG. 2

FIG. 1. Quartz mold for the growing of single-crystal samples of cylindrical form of specified crystallographic orientation: 1—sleeve with internal polished cylindrical surface, 2—common sleeve, 3—dismountable sleeve, 4—capillary with priming crystal of given orientation, 5—metal.

FIG. 2. Plot of  $X^{-1} \frac{\partial X}{\partial H}$  against  $H$  for a sample  $\text{SnI}^3$  with different surface quality (1–3) and for sample  $\text{KI}^3$  (4). The ordinate scale is indicated for curve 1. Curve 1 to the right of A, and the section of curve 2 in the vicinity of the SEC line, are magnified ten times; curve 3 is magnified 200 times. The value of  $X$  was determined from the change of the generation frequency, occurring when the sample goes over into a superconducting state,  $f = 4.6$  MHz, high-frequency field amplitude  $H_{\omega} = 6$  Oe, curves 1–3 were plotted for  $3.8^{\circ}\text{K}$ , curve 4 for  $1.7^{\circ}\text{K}$ . Curves 2–4 are shifted upward along the ordinate axis relative to curve 1. The horizontal straight lines determine the zero values of  $\partial X/\partial H$  for curves 2–4.

sitive to the surface quality. Figure 2 shows a plot of  $f'(H)$  of sample  $\text{SnI}^3$  (see the table) prior to etching (curve 1), after etching in nitric acid vapor (curve 2), and after deep etching in a special solution for the determination of the crystallographic orientation of the sample (curve 3). At a fixed crystallographic sample orientation, the quantity  $H^*$  at which a minimum (maximum) of the SEC line was observed was inversely proportional to the radius of the sample (Fig. 3). A similar change takes place in the position of the maximum and of the minimum of  $f'$  near a zero field (Fig. 3, there is no minimum on Fig. 3 owing to the large value of  $H_{\omega}$ , see above). If  $H$  is inclined at an angle  $\varphi$  to the cylinder axis, then the SEC lines and the non-monotonicity of  $X$  are influenced both by the value of  $\varphi$  and by the direction of  $H$  relative to the crystallographic axes of the sample. The SEC lines are observed only in a certain interval of angles and vary in a great variety of fashions: they split into two, with both components shifting towards large fields, or else the two shift in opposite directions; a case was observed when one component first shifted towards weaker fields and then, with further increase of  $\varphi$ , towards stronger fields; sometimes the line shifts without splitting into the direction of stronger (weaker) fields and to an equal degree for  $\pm\varphi$ , or else to stronger fields at  $+\varphi$  and in the opposite direction for  $-\varphi$ . The influence of the rotation of  $H$  on the minimum of  $f'$  near  $H = 0$  is manifest in a change of its depth and broaden-

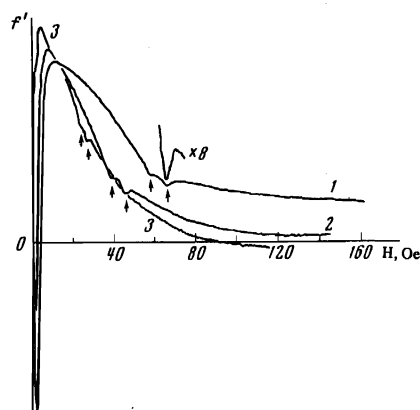


FIG. 3. Plot of  $f'(H)$  for tin cylinders of different dimension and the same crystallographic orientation: 1— $\text{SnI}^3$ , 2— $\text{SnI}^5$ , 3— $\text{Sn}2^8$ ,  $T = 4.2^{\circ}\text{K}$ .

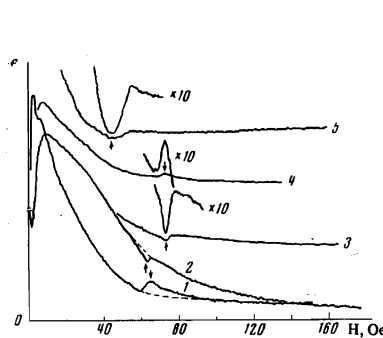


FIG. 4

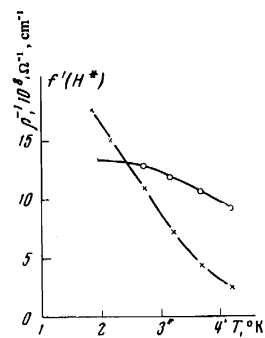


FIG. 5

FIG. 4. Plot of  $f'(H)$  of tin cylinders with different crystallographic orientations: 1— $\text{Sn}6^5$ , 2— $\text{Sn}8^5$ , 3— $\text{Sn}1^3$ , 4— $\text{Sn}5^3$ , 5— $\text{Sn}4^5$ ; curves 3–5 are shifted along the ordinate axis; the figure shows sections of curves 3–5 within the vicinity of the SEC lines, plotted with ten-fold magnification.

FIG. 5. Temperature dependence of the conductivity  $\rho^{-1}$  (O) and  $f'(H^*)$  (+) of sample  $\text{KI}^3$ . The quantity  $f'$  is plotted in arbitrary units.

ing, which were not equal for  $\pm\varphi$ . In all samples for which SEC was observed, with the exception of the etched  $\text{SnI}^3$ , a minimum of  $f'$  was observed near zero field, as well as a dependence of  $f'$  on  $H_{\omega}$ . Variation of the frequency in the range 1–10 MHz had little effect on  $f'(H)$ . With decreasing sample temperature, the intensity of all the lines increased.

To determine the connection between  $H^*$  and the topology of the Fermi surface, calibration measurements of  $f'(H)$  were made with a potassium sample. As is well known, the deviation of the Fermi surface of potassium from spherical is  $\lesssim 0.1\%$ , and  $p_F = 0.813$  g-cm/sec<sup>[11]</sup>. Unlike in<sup>[3]</sup>, we performed the measurements under the condition  $l \ll r$  (see the table). Figure 2 shows a plot of  $f'(H)$  for a potassium cylinder (curve 4). In contrast to<sup>[3]</sup>, we observed no singularities similar to size-effect lines. The quantity  $f'(H^*)$  depends strongly on the temperature. In Fig. 5 we show, for comparison, temperature dependences of  $f'(H^*)$  and of the conductivity of sample  $\text{KI}^3$  measured by the Sharvin-Zernov contactless induction method<sup>[12]</sup>. The change of frequency did not affect  $f'$  significantly. With an accuracy  $\approx 2\%$ , we obtain  $H^* = H_0 = p_F c / e r$ . If the magnetic field  $H$  makes an angle  $\varphi$  with the cylinder axis, then  $H^*$  shifts towards stronger fields:  $H^*(\varphi) \sim (\cos\varphi)^{-1/2}$ , and  $f'(H^*)$  decreases.

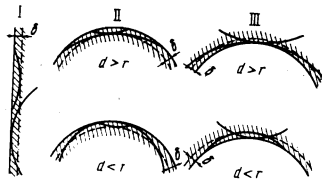


FIG. 6. Trajectories of electrons that form a high-frequency screening current in metallic samples of different geometrical form: I—half-space; II—cylinder; III—cavity. The shading shows the part of space filled with metal.  $H$  is perpendicular to the plane of the figure.

The ripples in  $\partial X/\partial H$ , of the SEC-line type, are a manifestation of a new size effect: a singularity is observed in the surface impedance of a metallic cylinder when the effective extremal radius of the electron trajectory becomes comparable in coordinate space with the radius of the sample. The physical nature of the cylinder can be easily understood. The screening high-frequency current in a metallic sample with a flat surface, placed in a constant magnetic field (we assume that the electron-trajectory radius is  $d \gg \delta$  and that  $\delta$  is sufficiently small), is produced by electrons of two types (see Fig. 6, I): (1) "surface" electrons, the trajectories of which lie entirely in the skin layer; (2) "volume" electrons, only a manageable fraction of whose trajectories lies in the skin layer. In the case of a cylindrical sample (Fig. 6, II) at  $r > d$ , the situation is analogous to the case of a sample with a flat surface, but when  $r < d$ , the "volume" electrons become "surface" electrons. In the case of a cylindrical cavity (Fig. 6, III) the situation is reversed, at  $d > r$  there are two types of "volume" electrons, and when  $d < r$  one of them becomes "surface."

In the case of specular reflection of the electrons from the sample surface ( $q = 1$ ), the skin layer is made up of "surface" electrons. In this case the field frequency dependences of the impedance have an unusual form:  $Z \sim \tau^{3/5} H^{-1/5}$  for a flat surface<sup>[13]</sup> and a cylinder at  $H \gg H_0$ <sup>[4]</sup>, which is in qualitative agreement with our measurements. The quasiperiodicity of the motion of the "surface" electrons at  $q = 0$  leads to the appearance of a system of electronic magnetic surface levels<sup>[14]</sup>, transitions between which cause the previously experimentally observed oscillations of the impedance of flat metallic plates in the microwave range in a weak magnetic field<sup>[15]</sup>, thus evidencing a noticeable contribution to the high-frequency current from the "surface" electrons that are specularly reflected by the surface of the sample. It is clear that the region  $d \approx r$  is singular. At  $q = 1$ , the singularity is due to the transformation of the "surface" electrons into "volume" electrons. At  $q = 0$ , the region is singled out by the fact that the effective meanfree path of the electrons in the skin layer,  $l_{\text{eff}}$ , is not limited by their collisions with the surface of the sample, is maximal, and is equal to  $l$ . The situation in which all the electrons in the middle move over circles of one radius takes place in the hypothetical case of a spherical Fermi surface. Somewhat more complicated, but realized to a high degree of accuracy in potassium and sodium, is the case of a spherical Fermi surface. As shown by calculations<sup>[4]</sup>, in the case of a quadratic dispersion law the singularity in  $Z$  and  $H \approx H_0$  should become manifest both at  $q = 1$  and at  $q = 0$ . However, the mechanisms that bring about the singularity in these two cases are different. At  $q = 1$ , with decreasing  $H$ , the electrons on the central

section of the Fermi surface, which make an appreciable contribution to the high-frequency current, become transformed at  $H \approx H_0$  from "volume" into "surface" electrons, as the result of which a singularity appears in  $Z$ . At  $z = 0$ , the main contribution to the high-frequency current is made by electrons travelling parallel to the sample surface, and having  $l_{\text{eff}} \approx l$ . At  $H < H_0$ , these are the electrons from a narrow belt on the Fermi surface, whose trajectories in coordinate space are circles in a plane perpendicular to  $H$ , ( $r - \delta < d < r$ ). With increasing  $H$ , their number increases continuously and becomes anomalously large at  $H \approx H_0$ , when electrons of the central cross section of the Fermi surface move parallel to the surface, as the result of which a singularity should be observed in  $Z$  near  $H_0$ . The results of our measurements with the potassium cylinder (Fig. 2, curve 4) are in qualitative agreement with theoretical calculations<sup>[4]</sup>, assuming  $q \neq 0$ .

We can summarize the foregoing in the following manner. In a longitudinal magnetic field, a singularity should be observed at  $H \approx H_0$  in the  $Z(H)$  dependence of a metallic cylinder with a cylindrical Fermi surface whose axis is directed along the axis of the sample, or with a spherical Fermi surface. This singularity is due to the following causes: At  $q = 0$ , it is due to the anomalously large number of the electrons forming the skin layer (the Fermi surface is a sphere,  $l_{\text{eff}} = \text{const}$ ), or to the maximum value of  $l_{\text{eff}}$  (the Fermi surface is a cylinder, the number of the effective electrons is constant). At  $q = 1$ , the singularity is due to the transformation of the surface electrons of the extremal section of the Fermi surface into volume electrons. The curvature of the intersection of the Fermi surface by a plane passing through its symmetry axis does not determine the critical condition for the existence of SEC, and the arguments at least are valid for any axially-symmetrical Fermi surface with a symmetry axis directed along the sample axis. In this case the singularity in  $Z(H)$  is due to electrons of the strip of extremal cross section of the Fermi surface. In the case of an arbitrary dispersion law, the Fermi surface can have "pieces" of extremal-section strips, which are axially symmetrical to the Fermi surface, or else effective sections of Fermi surface that determine the singularity of the impedance of the corresponding regions of the sample, and consequently of the impedance of the entire metallic cylinder. The fact that large effective sections exist in the Fermi surface of tin for certain directions is indeed the reason for the observation of singularities in the impedance of tin cylinders of the SEC-line type.

The geometry of the effective section of the Fermi surface determines the shape, width, and line intensity of the SEC. In the case of a spherical Fermi surface, the line constitute an intense broad peak in  $\partial X/\partial H$ , which is not symmetrical about the maximum, and the position of which is determined by the sample diameter (see<sup>[3]</sup> and curve 4 of Fig. 2). The SEC line has a similar shape in indium<sup>[5]</sup>, because the Fermi surface of indium has spherical "pieces" whose areas make up, as is well known, an appreciable fraction of the total area of the Fermi surface, and apparently it is the electrons from just these regions that make the main contribution to the magnetic-field-dependent part of  $Z$ . In tin cylinders, the SEC lines constitute relatively narrow ripples, minima, and maxima (see Figs. 3–4). At a fixed crystallographic orientation, in samples with approximately equal surface quality, the product of the width of the

SEC line by  $r$  is constant (Fig. 3). At the same time, the surface quality can greatly influence the width of the line (cf. curves 1 and 2 of Fig. 2). The factor that determines the type of the extremum of the SEC line is still not clear. Its independence of  $r$  (Fig. 3), of the temperature, and of the surface quality (Fig. 2) favors a dominant influence of the geometry of the effective section of the Fermi surface. We note that the minima and maxima have different line shapes, as can be clearly seen on the most intense lines (curves 1, 2 of Fig. 4).

A study of the position of the SEC line on the  $H$  axis, of its shape, of its intensity, and of its change when  $H$  is inclined at an angle to the sample axis, with decreasing temperature, the dependence on the frequency of the electromagnetic field, can all give information on the topology of the Fermi surface and on the interaction of the electrons with the surface of the metal. To this end, however, it is necessary to carry out an appropriate theoretical calculation. The most obvious use of the SEC is for the determination of the intersection of the effective Fermi-surface section with a plane perpendicular to  $H$ . Here, however, it is necessary to bear in mind the following circumstance. It has been experimentally established that if  $H$  makes an angle with the sample axis, then the SEC lines are observed in a certain angle interval. On the other hand, if the "axial axis" of the effective section of the Fermi surface is directed at an angle to the cylinder axis, then an SEC line should be observed, apparently just when  $H$  is inclined to the cylinder axis which coincides with the axial axis of the effective section of the Fermi surface. This leads to difficulties in the determination of the position of the effective section on the Fermi surface.

A systematic study of the geometry of the Fermi surface of tin was not the task of the present paper, but from the obtained experimental data we can draw certain conclusions. According to the model of almost-free electrons we have in tin  $p_F^0 = 1.73 \times 10^{-19}$  g-cm/sec. It is seen from the table that the values of the curvature radii obtained from the SEC differ insignificantly from  $p_F^0$ , with the exception of the case of samples Sn6<sup>5</sup> and Sn8<sup>3</sup>, thus indicating that the Fermi surface of tin has regions with curvature radii close to  $p_F^0$ . The weak intensity of the SEC line in the Sn5<sup>3</sup> sample, the direction of the axis of which is close to the direction of the [001] axis, indicates that in the extremal intersections of the Fermi surface of tin with the plane (001) there are few sections of constant temperature. According to the known structure of the Fermi surface of tin, it is natural to assume that the main contribution to the line intensity of the sample Sn5<sup>3</sup> will be made by electrons from a strip of the central section of the almost cylindrical part of the Fermi surface, with axis along [001] in the fourth zone, or more accurately, of the vicinities of this strip near the points of intersection of the Fermi surface with the axes [100] and [1010]. In [16], a Gaussian curvature  $K^{-1/2} = 2.31 \times 10^{-19}$  g-cm/sec was obtained for the limiting point at  $H$  directed along [100]. Using this value and the data on the SEC in the Sn5<sup>3</sup> sample, we obtain for the curvature radius of the extremal section of the Fermi surface with a plane containing the [001] axis a value  $2.8 \times 10^{-19}$  g-cm/sec, which is close to the SEC data for samples Sn6<sup>5</sup> and Sn8<sup>3</sup>. There are no grounds, however, for concluding that the SEC lines in the samples Sn6<sup>5</sup> and Sn8<sup>3</sup> are due to the region of the limiting point of the Fermi-surface strip of the indicated section, as is indicated,

in particular, by the fact we were unable to observe SEC in a sample with an axis directed along the [100] axis.

The available experimental data do not suffice to explain the physical nature of the nonmonotonic and nonlinear dependence of  $Z(H)$  near  $H = 0$ , although the influence of the size of the radius of the sample on  $Z(H)$  is subject to no doubt (see Fig. 3). This allows us to conclude that the previously observed nonmonotonic dependence of  $Z(H)$  of tin cylinders<sup>[2]</sup> is connected with the size of the sample radius. There are two most probable causes of the non-monotonicity and nonlinearity of  $Z(H)$ : (1) The SEC on the sections of the Fermi surface with small curvature radius, the form of curves 1 and 2 in Fig. 3 in general terms coincide with the form of curve 4 of Fig. 2, which was obtained with a potassium cylinder; (2) the appearance of a system of magnetic surface levels, which should lead to a nonlinearity in the non-monotonicity of  $Z(H)$ <sup>[17,18]</sup>. The cylindrical character of the sample surface leads to a quasiperiodic motion of the electrons, and at  $H = 0$  it leads to the appearance of quantum surface states in a zero field<sup>[19]</sup>.

To explain the physical nature of the non-monotonicity and the nonlinearity of  $Z(H)$  and to study the SEC, it is of interest to perform experiments on cylindrical cavities. In this case the system of magnetic surface levels can occur only at  $H > H_0$ , just where the singularities of  $Z(H)$  should appear. Unlike a cylinder, in a cavity, when  $H$  exceeds  $H_0$ , the extremal electrons turn from "volume" type into "surface" type.

The author is grateful to V. F. Gantmakher for a discussion of the results.

<sup>1</sup>B. É. Meřerovich, Zh. Eksp. Teor. Fiz. 57, 1445 (1969) [Sov. Phys.-JETP 30, 782 (1970)].

<sup>2</sup>V. F. Gantmakher and Yu. V. Sharvin, Zh. Eksp. Teor. Fiz. 39, 512 (1960) [Sov. Phys.-JETP 12, 358 (1961)].

<sup>3</sup>T. G. Blaney, Phil. Mag. 20, 23 (1969).

<sup>4</sup>B. É. Meřerovich, Zh. Eksp. Teor. Fiz. 59, 276 (1970) [Sov. Phys.-JETP 32, 149 (1971)].

<sup>5</sup>V. S. Tsoi, ZhETF Pis. Red. 15, 246 (1972) [JETP Lett. 15, 171 (1972)].

<sup>6</sup>V. F. Gantmakher, Zh. Eksp. Teor. Fiz. 42, 1416 (1962) [Sov. Phys.-JETP 15, 982 (1962)].

<sup>7</sup>Yu. V. Sharvin and V. F. Gantmakher, Prib. Tekh. Eksp. No. 6, 165 (1963).

<sup>8</sup>V. S. Tsoi and V. F. Gantmakher, Zh. Eksp. Teor. Fiz. 56, 1232 (1969) [Sov. Phys.-JETP 29, 663 (1969)].

<sup>9</sup>R. G. Chambers, Nature, 165, 239 (1950).

<sup>10</sup>V. F. Gantmakher, Zh. Eksp. Teor. Fiz. 44, 811 (1968) [Sov. Phys.-JETP 17, 549 (1968)].

<sup>11</sup>D. Shoenberg, P. L. Stiles, Prob. Roy. Soc. A281, 62 (1964).

<sup>12</sup>V. B. Zernov and Yu. V. Sharvin, Zh. Eksp. Teor. Fiz. 36, 1038 (1959) [Sov. Phys.-JETP 9, 737 (1959)].

<sup>13</sup>E. A. Kaner and N. M. Makarov, Zh. Eksp. Teor. Fiz. 57, 1435 (1969) [Sov. Phys.-JETP 30, 772 (1970)].

<sup>14</sup>Tsu-WeiNee, R. E. Prange, Phys. Lett. 25A, 582 (1967).

<sup>15</sup>M. S. Khařkin, Zh. Eksp. Teor. Fiz. 39, 212 (1960)

- [Sov. Phys.-JETP 12, 152 (1961)].
- <sup>16</sup>V. F. Gantmakher and E. A. Kaner, Zh. Eksp. Teor. Fiz. 45, 1430 (1963) [Sov. Phys.-JETP 18, 988 (1964)].
- <sup>17</sup>M. S. Khaikin, Usp. Fiz. Nauk 96, 409 (1968) [Sov. Phys.-Usp. 11, 785 (1969)].
- <sup>18</sup>V. F. Gantmakher, L. A. Fal'kovskiĭ, and V. S. Tsoĭ, ZhETF Pis. Red. 9, 246 (1968) [JETP Lett. 9, 144 (1968)].
- <sup>19</sup>R. E. Prange, Phys. Rev. 171, 737. 1968.

Translated by J. G. Adashko  
227